Copy 6
RM L53K20a

NACA RM L53K20a

RESEARCH MEMORANDUM

COMPARISON OF EXPERIMENTAL HYDRODYNAMIC IMPACT LOADS AND MOTIONS FOR A V-STEP AND A TRANSVERSE-STEP HYDRO-SKI

By Robert W. Miller

Langley Aeronautical Laboratory
Langley Field, Va.

CLASSIFICATION CHANGED

To UNCLASSIFIED

By authority of Naca RA + RN-112 Effective Date 2-8-57
NB 3-12-57

CLASSIFIED DOCUMENT

This material contains information affecting the National Defense of the United States within the meaning of the espionage laws, Title 18, U.S.C., Secs. 793 and 794, the transmission or revelation of which in any manner to an unauthorized person is prohibited by law.

LIBRARY COPY
FEB 4 1954
LANGLEY AERONAUTICAL LABORATORY
LIBRARY, NACA
LANGLEY FIELD, VIRGINIA

NATIONAL ADVISORY COMMITTEE
FOR AERONAUTICS

WASHINGTON
February 2, 1954

NASA Technical Library
3 1176 01437 6041

NATIONAL ADVISORY COMMITTEE FOR AERONAUTICS

RESEARCH MEMORANDUM

COMPARISON OF EXPERIMENTAL HYDRODYNAMIC IMPACT LOADS AND MOTIONS FOR A V-STEP AND A TRANSVERSE-STEP HYDRO-SKI

By Robert W. Miller

SUMMARY

A comparison is presented of the hydrodynamic impact loads and motions encountered in testing a V-step and a transverse-step flat-bottom hydro-ski having beam loadings of about 4.5. The tests were made in smooth water over a range of velocities, flight-path angles, and fixed trims.

The data were obtained as time histories of draft, vertical velocity, and vertical acceleration and the comparisons are presented as plots of the nondimensional load, draft, vertical velocity, and time coefficients at maximum load, maximum draft, and rebound against flight-path angle at contact. The results show that the V-step reduces maximum impact loads up to 50 percent, increases the depth of penetration, and changes some of the vertical velocity and time characteristics of the hydro-ski.

INTRODUCTION

The possibility of reduction of hydrodynamic impact loads on hydro-skis by the use of V-step configurations is of current interest in the design of high-speed water-based aircraft. It is therefore desirable to provide an illustration of the amount of this load reduction obtainable over a range of flight-path angle and trim which is of primary interest to the designer.

Test results for a V-step and a transverse-step flat-bottom hydro-ski have been published in references 1 and 2, respectively. The tests of the V-step model were made at trims of 4°, 12°, and 20°, and initial flight-path angles ranging from 2.7° to 20.7°. The tests of the transverse-step model were made at trims of 3°, 9°, and 15°, and initial flight-path angles from 2.3° to 11.5°. The beam-loading coefficients of these two skis were practically the same (4.6 and 4.4); thus, a direct comparison is possible. The purpose of the present paper is to present this comparison of the hydrodynamic impact loads and motions, at the maximum load, maximum draft, and rebound encountered in testing the

[redacted]

V-step and transverse-step hydro-skis and to show the reduction of maximum loads obtained by use of the V-step.

SYMBOLS

b	beam of model, ft
F_z	vertical hydrodynamic force, lb
g	acceleration due to gravity, 32.2 ft/sec^2
m	mass of model, slugs
n_{i_w}	impact load factor, F_z/mg or $\ddot{z}/g$
t	time after water contact, sec
V	resultant velocity, ft/sec
W	weight, lb
z	model draft, ft
$\dot{z}$	vertical velocity of model, ft/sec
$\ddot{z}$	vertical acceleration of model, ft/sec^2
γ	flight-path angle, deg
ρ	mass density of water, 1.938 slugs/cu ft
τ	trim, deg

Dimensionless variables:

C_Δ	beam loading coefficient, $m/\rho b^3$
C_d	draft coefficient, z/b
C_L	impact lift coefficient, $F_z\Big/\frac{1}{2}\rho b^2 {V_o}^2$
C_t	time coefficient, $V_o t/b$

Subscripts:

o at time of water contact

max maximum

APPARATUS AND TEST PROCEDURE

Apparatus.- The tests were conducted in the Langley impact basin with the test equipment described in reference 3.

The V-step model used was essentially a rigid flat plate having a rectangular forward portion and a triangular aft portion with a 2:1 taper ratio and a C_Δ of 4.6. A sketch showing the shape and dimensions of this model is given in figure 1(a).

The transverse-step model was described in reference 2. It had a beam of 20 inches which, at the dropping weight used, resulted in a C_Δ of 4.4. A sketch showing its shape and dimensions is given in figure 1(b).

Instrumentation.- The standard carriage instrumentation, described in reference 3, was used to measure time histories of the lift force and of the horizontal and vertical components of velocity and displacement. Accelerations in the vertical direction were measured by an unbonded strain-gage-type accelerometer which had a natural frequency of 105 cps and was oil damped to about 65 percent of the critical damping.

The apparatus and instrumentation used gave measurements that are believed to be accurate within the following limits:

Horizontal velocity, ft/sec	±0.5
Vertical velocity at contact, ft/sec	±0.2
Vertical displacement, ft	±0.03
Acceleration, g	±0.2
Time, sec	±0.005
Weight, lb	±2.0

Test procedure.- The V-step model was tested at trims of 4°, 12°, and 20°. The initial horizontal velocity for these tests was varied from approximately 25 ft/sec to 85 ft/sec, and the vertical velocity at water contact was varied from approximately 4 ft/sec to 10 ft/sec. The total dropping weight of the model and drop linkage was 1330 pounds.

The transverse-step-model tests were conducted at trims of 3°, 9°, and 15° with horizontal velocities between 41 and 51 ft/sec and vertical velocities between 2 and 9 ft/sec. The dropping weight of the transverse-step model was 1261 pounds.

Throughout each impact a simulated aerodynamic lift force equal to the total dropping weight was exerted on the model by means of the lift engine. The lift engine and general testing procedure used are described in reference 3.

RESULTS AND DISCUSSION

The experimental data were obtained from the tests as time histories of draft, vertical velocity, and vertical acceleration. The values of initial conditions and the recorded data at maximum acceleration, maximum draft, and rebound are given in tables I and II. The V-step-model data (table I) were presented in reference 1 and are repeated here for the convenience of the reader. The transverse-step-model data (table II) were partly presented in reference 2. The remainder were obtained directly from the records and have not been previously published.

The results of the tests are presented as plots of the nondimensional coefficients $C_{L_{max}}$, C_d, $\dot{z}/\dot{z}_o$, and C_t with flight-path angle at water contact. The plots are arranged to show the comparison in both magnitude and trends between the V-step-model and the transverse-step-model results either as a direct or side-by-side comparison.

Figure 2 presents the variation of impact-lift coefficient at the instant of maximum acceleration with flight-path angle at the instant of water contact for both models. For both models, the value of impact lift coefficient increases with flight-path angle. It decreases slightly with increasing trim except that, below a flight-path angle of about 7°, the trend with trim is reversed for the transverse-step model. Figure 2 shows that, in general, the V-step hydro-ski has smaller maximum hydrodynamic load than the transverse-step model. The greatest reduction of the maximum load, up to 50 percent, is to be found at the high-trim, low-flight-path-angle conditions with some tendency for the curves to merge at the high-flight-path angles where the rectangular portion of the V-step hydro-ski would become immersed. However, a considerable reduction of maximum load does occur over most of the range of conditions tested.

Figure 3 presents the draft coefficient at the instant of maximum immersion and also at the instant of maximum acceleration plotted against flight-path angle at water contact for both models. From comparison of the plots for the two models it can be seen that, in general, the V-step model has a much greater depth of penetration both at the time of maximum acceleration and at maximum immersion than does the transverse-step model. The draft coefficient increases with increasing flight-path angle for both models at both the times illustrated. It increases also with trim for the V-step model at both times and for the transverse-step model at the instant of maximum acceleration. However, for the transverse-step model at the instant of maximum immersion, the trend with trim is reversed, that is, the greater immersions occur at the smaller trims. At the low-trim, high-flight-path-angle conditions, bow immersion was encountered by both models. However, this immersion does not appear to have had any appreciable effect on the results.

In figure 4 the ratios of the vertical velocities at the instant of maximum acceleration and at the instant of model rebound to the vertical velocity at water contact are plotted against flight-path angle at water contact for both models. In general, there are no large differences between the two models in regard to vertical velocity ratios.

Figure 4 shows that, for a given contact velocity, the vertical velocity at maximum acceleration increases with increases in contact flight-path angle and decreases with increasing trim. At the lower flight-path angles, where the effect of the V-portion of the model is greatest, the V-step model has somewhat lower vertical velocity ratios than the transverse-step model. On the other hand, at the higher flight-path angles, where the effect of the rectangular portion becomes more pronounced, the ratios for the two models are of about the same magnitude. Thus, the V-portion of the model appears to reduce the vertical velocity at maximum acceleration but, as the effect of the rectangular portion of the model becomes more pronounced, the ratios approach those of the transverse-step model.

At rebound, for a given contact velocity, the absolute value of the vertical velocity decreases with increasing contact flight-path angle and increases with trim for both models. It appears that the effect of the V-step is to reduce the slope of the curves at the lower flight-path angles and to increase the slope of the curves at the higher angles but the effect is not pronounced.

Figure 5 shows the effect of trim and flight-path angle at water contact upon the time to reach maximum acceleration, to reach maximum draft, and for model rebound for both models. Figure 5 shows that there is more difference between the two models in regard to the time coefficient than has been the case for the quantities previously discussed.

The time coefficient at maximum acceleration decreases with increasing flight-path angle but increases with trim for both models. The values of the coefficient for the transverse-step model (about 0.3 to 2.0), however, are much smaller than for the V-step model (about 1.4 to 9.0) and show that the V-step retards maximum acceleration until considerably later in the impact.

At the time of maximum immersion the trends of the time coefficient with flight-path angle and trim are exactly opposite for the two models.

For the V-step model, the time coefficient decreases with increasing flight-path angle and increases with trim whereas for the transverse-step model it increases with flight-path angle and decreases with increasing trim. The values, however, lie in the same general range so that the maximum immersion for the two models occurs at about the same part of the impact. For both models the time coefficients for maximum acceleration and for maximum immersion appear to be converging with decreasing flight-path angle; thus, for very small flight-path angles, maximum acceleration would occur at approximately the time of maximum immersion. This tendency is apparent for both models but is much more pronounced for the V-step model.

The time coefficient at rebound, for the V-step model, appears initially to decrease and then to increase with increasing flight-path angle and at the lower flight-path angles it increases with trim whereas at the higher flight-path angles it decreases with increasing trim. On the other hand, for the transverse-step model, no reversal of trends is present; the coefficient increases with flight-path angle and decreases with increasing trim.

CONCLUSIONS

A comparison was made of experimental data for hydrodynamic impacts of a V-step and a transverse-step hydro-ski having beam loading coefficients of 4.6 and 4.4, respectively. The data were compared, in nondimensional coefficient form, either directly or in side-by-side plots. The comparison has resulted in the following conclusions:

1. The V-step reduces the maximum impact loads up to 50 percent, at least, at the lower flight-path angles.

2. The V-step model has a greater depth of penetration than does the transverse-step model.

3. The V-step tends to reduce the vertical velocity at the time of maximum acceleration.

4. The V-step retards the time of maximum acceleration so that it approaches the time of maximum penetration.

Langley Aeronautical Laboratory,
National Advisory Committee for Aeronautics,
Langley Field, Va., November 6, 1953.

REFERENCES

1. Miller, Robert W.: Water-Landing Investigation of a Flat-Bottom V-step Model and Comparison With a Theory Incorporating Planing Data. NACA TN 2932, 1953.

2. Batterson, Sidney A.: Water Landing Investigation of a Hydro-Ski Model at Beam Loadings of 18.9 and 4.4. NACA RM L51F27, 1951.

3. Batterson, Sidney A.: The NACA Impact Basin and Water Landing Tests of a Float Model at Various Velocities and Weights. NACA Rep. 795, 1944. (Supersedes NACA WR L-163.)

TABLE I

DATA FROM TESTS OF A V-STEP HYDRO-SKI

$W = 1330$ pounds; $C_{\Delta} = 4.6$

Run	τ, deg	At contact -				At $(n_{i_w})_{max}$ -				At z_{max} -		At rebound -	
		V_o, fps	$\dot{x}_o$, fps	$\dot{z}_o$, fps	γ_o, deg	t, sec	n_{i_w}, g	z, ft	$\dot{z}$, fps	t, sec	z, ft	t, sec	$\dot{z}$, fps
1	4	75.6	75.4	5.8	4.4	0.053	2.4	0.28	4.8	0.138	0.41	0.389	-2.2
2	4	73.1	72.7	7.9	6.2	.043	3.3	.31	6.8	.130	.52	.430	-2.4
3	4	60.2	59.5	8.9	8.5	.040	3.8	.31	7.9	.145	.62	.585	-2.2
4	12	84.8	84.8	4.1	2.7	.140	1.3	.41	1.8	.170	.42	.377	-2.7
5	12	77.2	76.9	6.1	4.6	.124	2.1	.56	2.8	.149	.59	.355	-3.8
6	12	74.3	73.8	8.1	6.4	.102	3.1	.65	4.1	.139	.71	.349	-4.5
7	12	54.5	53.8	8.9	9.4	.095	2.7	.70	5.9	.170	.86	.462	-3.9
8	12	48.0	47.1	9.4	11.3	.089	2.4	.74	6.8	.174	.95	.544	-3.6
9	12	38.7	37.5	9.6	14.3	.093	2.2	.77	7.0	.210	1.08	.725	-2.6
10	20	83.8	83.7	4.5	3.0	.174	1.3	.54	1.4	.189	.54	.420	-3.3
11	20	73.2	72.8	7.7	6.1	.147	2.9	.84	2.6	.172	.84	.380	-5.7
12	20	47.3	46.2	10.0	12.2	.129	2.5	1.06	6.1	.203	1.20	.535	-5.0
13	20	35.9	34.5	9.9	16.0	.140	1.9	1.12	6.4	.270	1.39	.716	-3.4
14	20	25.9	24.3	9.2	20.7	.150	1.4	1.14	6.7	.330	1.60	1.170	-1.8

TABLE II

DATA FROM TESTS OF A TRANSVERSE-STEP HYDRO-SKI

[W = 1261 pounds; C_{Δ} = 4.4]

Run	τ, deg	At contact -				At $(n_{i_w})_{max}$ -				At z_{max} -		At rebound -	
		V_o, fps	$\dot{x}_o$, fps	$\dot{z}_o$, fps	γ_o, deg	t, sec	n_{i_w}, g	z, ft	$\dot{z}$, fps	t, sec	z, ft	t, sec	$\dot{z}$, fps
1	3	48.8	48.8	2.2	2.52	0.030	.5	0.058	1.59	0.215	0.13	0.457	-0.48
2	3	50.1	49.8	4.9	5.66	.016	1.7	.034	4.86	.246	.33	.790	-.96
3	3	42.5	42.0	6.2	8.42	.015	2.0	.106	5.66	.345	.55	1.180	-.48
4	3	42.4	41.9	6.3	8.55	.013	2.0	.091	5.98	.348	.52	1.215	-.16
5	3	43.1	42.2	8.6	11.53	.013	2.8	.083	7.81	.343	.75	1.153	-.96
6	9	50.5	50.4	2.1	2.35	.034	.9	.060	1.67	.130	.10	.250	-1.35
7	9	50.1	49.9	4.8	5.48	.032	1.6	.147	3.99	.153	.29	.342	-2.55
8	9	51.2	51.0	5.0	5.62	.030	1.8	.137	4.30	.143	.27	.335	-2.31
9	9	42.9	42.5	6.1	8.12	.032	1.9	.266	5.66	.167	.46	.467	-.48
10	9	44.0	43.5	6.2	8.13	.034	1.8	.262	4.70	.192	.44	.465	-2.31
11	9	42.8	42.1	8.1	10.84	.036	2.4	.230	7.01	.176	.55	.506	-2.55
12	9	43.8	43.0	8.4	11.02	.031	2.5	.228	7.49	.194	.58	.504	-2.55
13	15	50.0	50.0	2.0	2.28	.058	1.0	.078	1.20	.105	.10	.224	-1.83
14	15	50.2	50.0	4.9	5.55	.047	1.8	.183	3.67	.118	.28	.285	-3.51
15	15	43.7	43.3	6.2	8.18	.053	1.9	.253	4.62	.159	.39	.365	-3.35
16	15	43.7	42.9	8.5	11.15	.041	2.4	.265	6.69	.161	.50	.410	-3.83

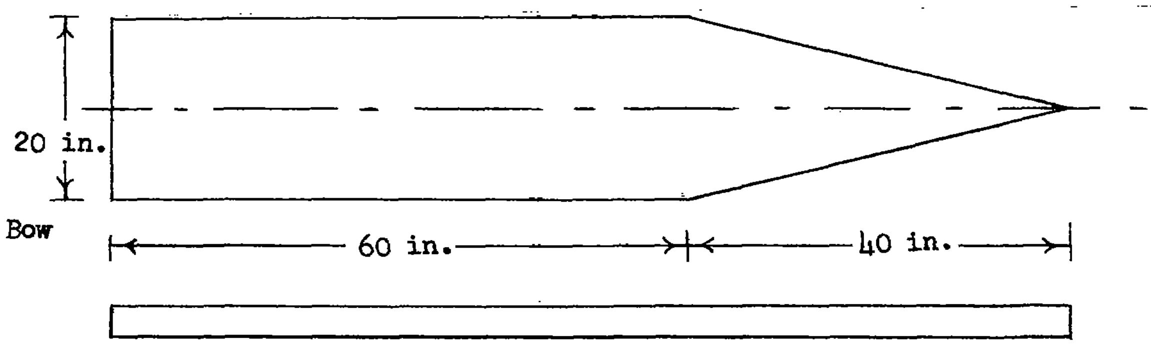

(a) Flat bottom, V-step model. W = 1330 lb.

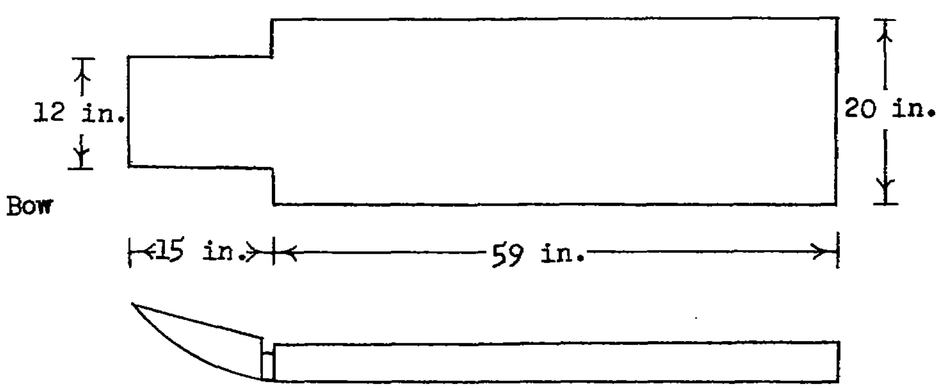

(b) Flat bottom, transverse-step model. W = 1261 lb.

Figure 1.- Models tested in Langley impact basin.

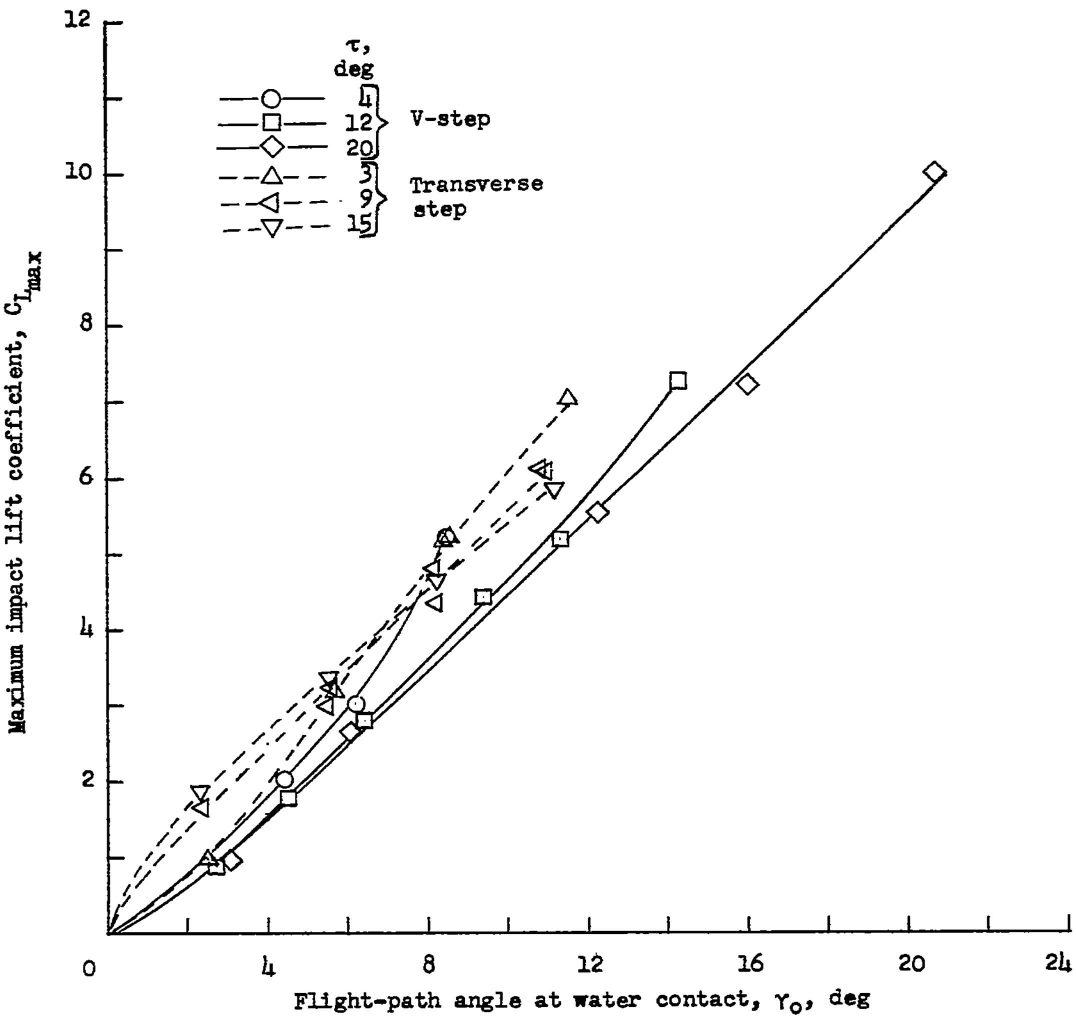

Figure 2.- Variation of impact lift coefficient at instant of maximum acceleration with flight-path angle at water contact.

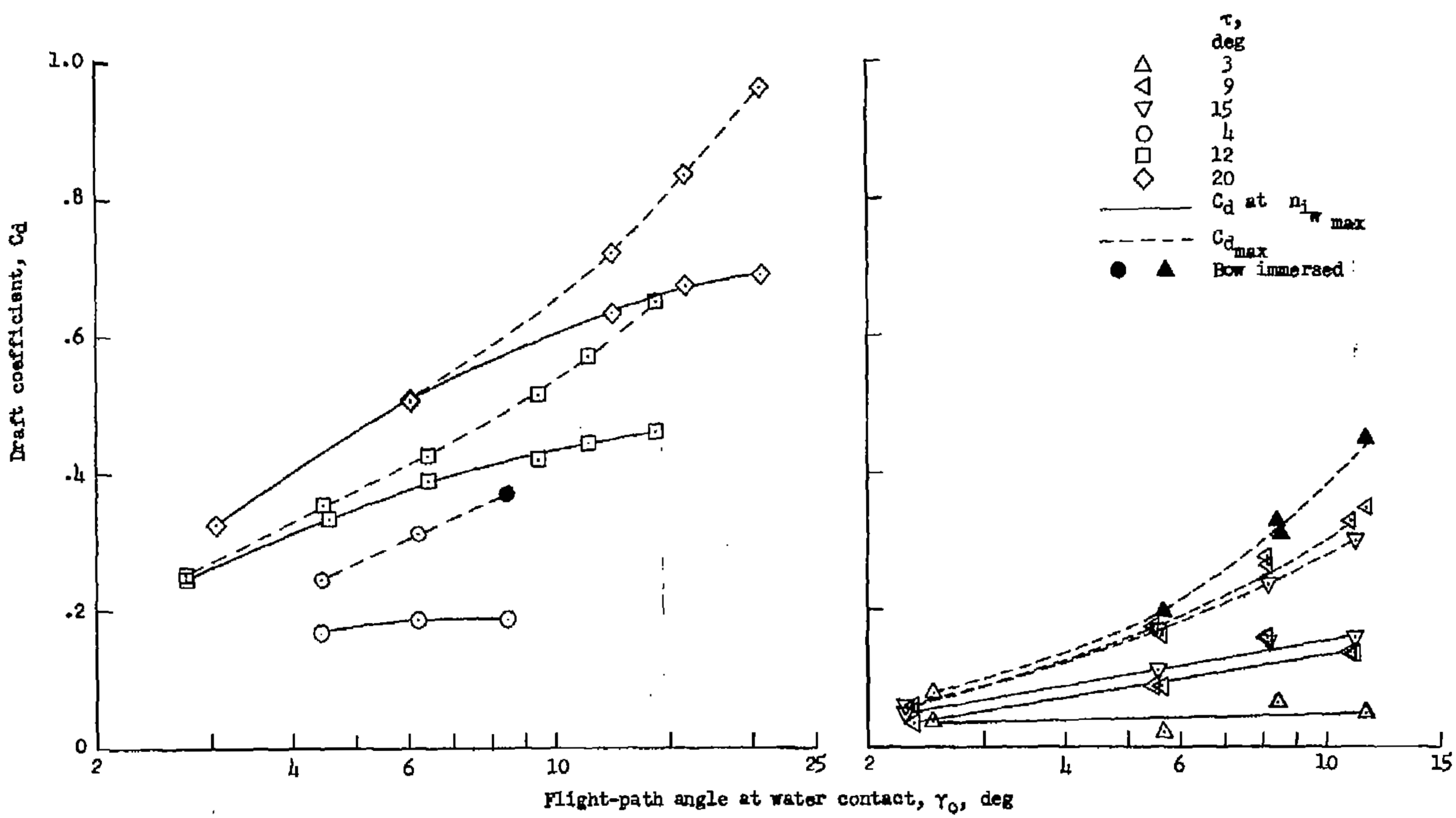

(a) V-step model. (b) Transverse-step model.

Figure 3.- Variation of draft coefficient with flight-path angle at water contact.

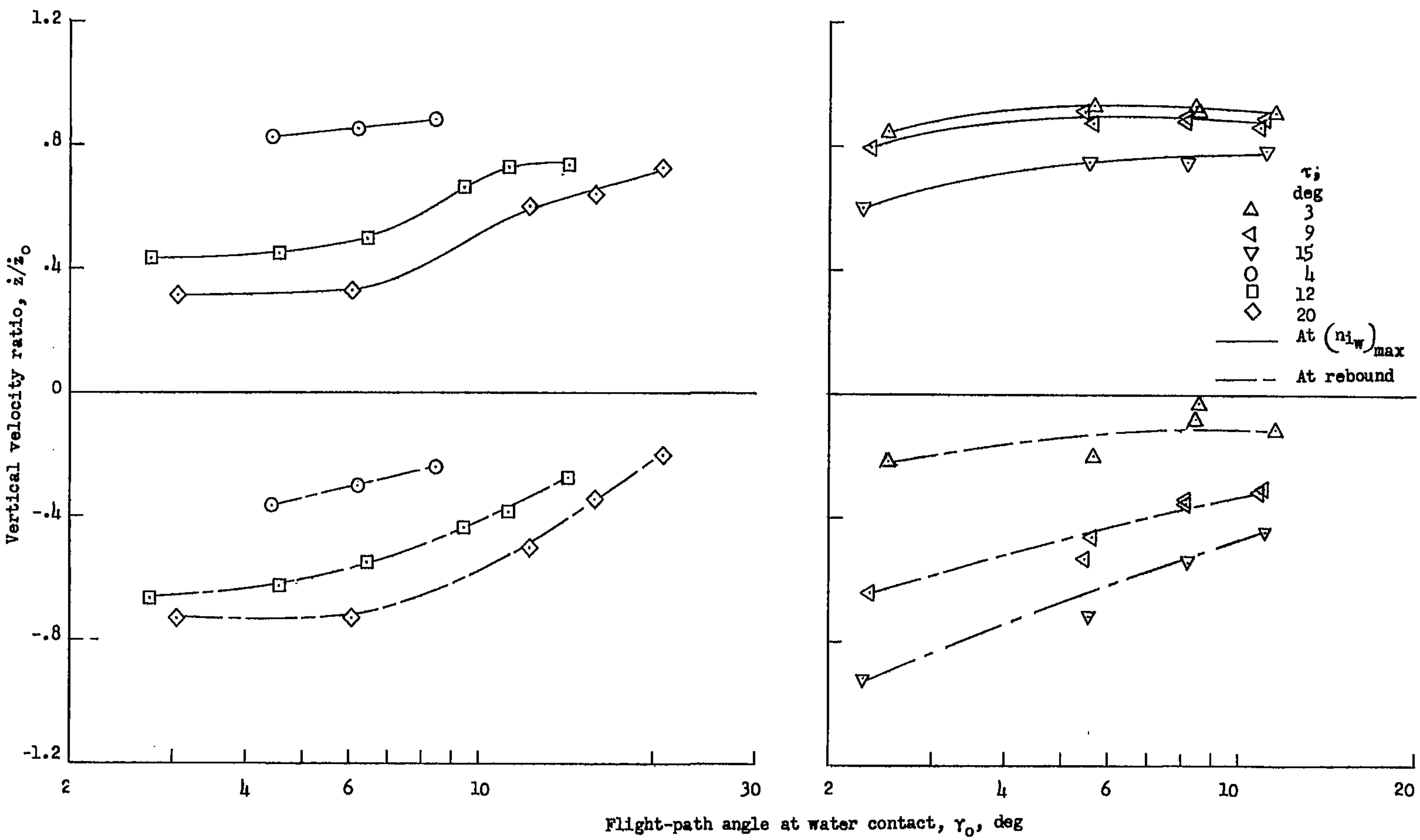

(a) V-step model. (b) Transverse-step model.

Figure 4.- Variation of vertical-velocity ratio at maximum acceleration with flight-path angle at water contact.

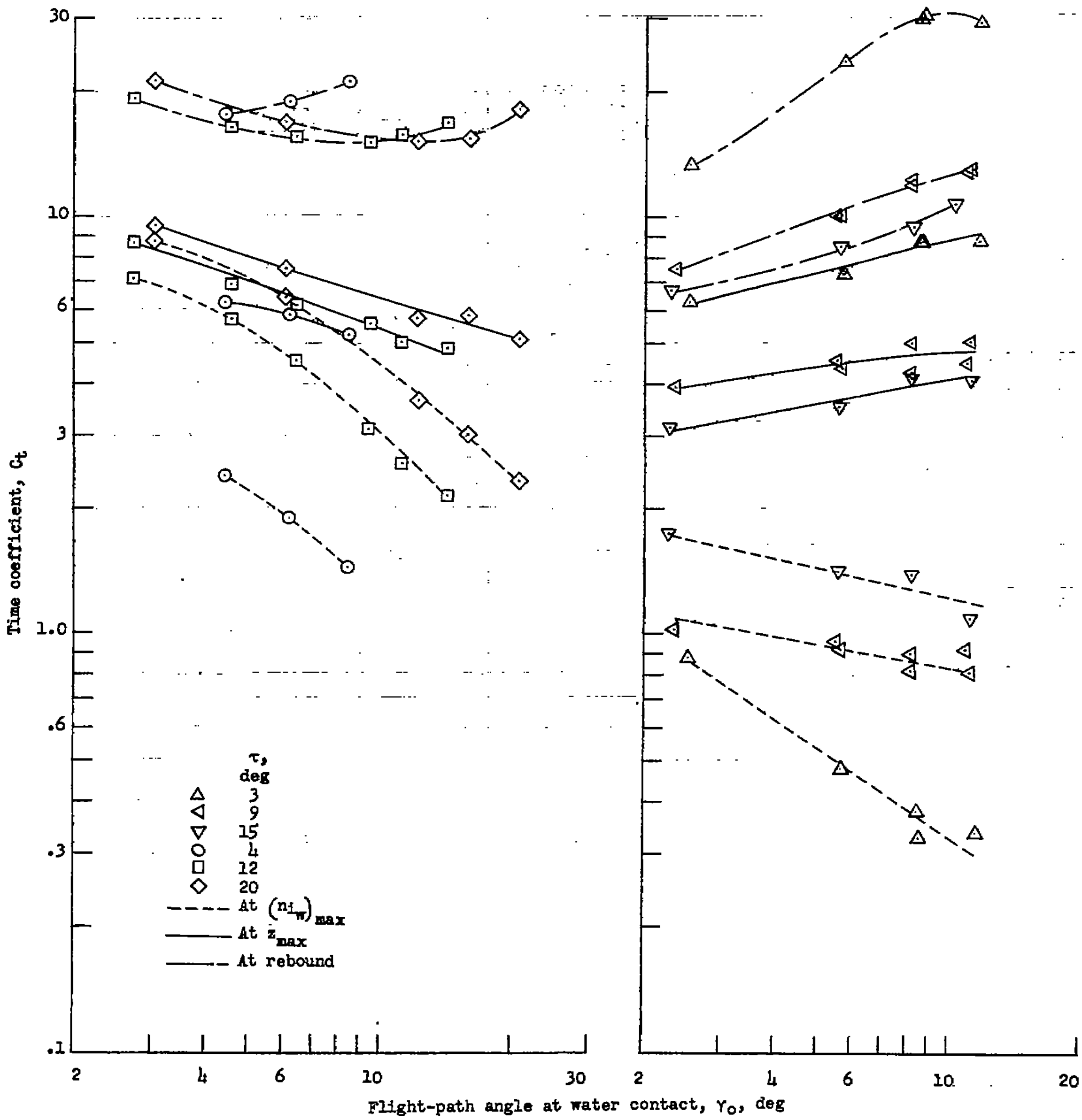

(a) V-step model. (b) Transverse-step model.

Figure 5.- Variation of time coefficient with flight-path angle at water contact.

[redacted]

NASA Technical Library
3 1176 01437 6041

[redacted]